Electronic scattering from Co/Cu interfaces: *In situ* measurement and comparison with theory

William E. Bailey*
Department of Materials Science & Engineering, Stanford University, Stanford, California 94305-2205

Shan X. Wang†
Department of Materials Science & Engineering, Stanford University, Stanford, California 94305-2205
and Department of Electrical Engineering, Stanford University, Stanford, California 94305-4035

Evgueni Yu. Tsymbal
Department of Materials, University of Oxford, Parks Road, Oxford OX1 3PH, United Kingdom
(Received 12 May 1999)

The full thickness-dependent electrical conductivity of polycrystalline NiO/Co/Cu/Co spin-valve structures was measured *in situ* during ion-beam deposition and compared with calculations based on realistic band structure. We have found striking features in the experimental conductivity which are unexpected from widely used semiclassical free-electron models. Addition of ~1 ML Co to a NiO/Co/Cu surface causes the net film conductance to decrease; the reverse case of Cu on NiO/Co shows a strong positive curvature of the thickness-dependent conductance, indicating a reduction of the conductivity in Cu near the interface with Co. Quantitative agreement is found between the experimental thickness-dependent film conductance and multiband tight-binding model calculations using a single constant parameter for on-site atomic disorder. The experimental data are consistent with strong scattering of conduction electrons in Cu at the interfaces with Co. Comparison with theory suggests that most of the observed interface scattering may be considered to be intrinsic, arising from the placement of a high density of empty Co *d* states at the Cu boundaries.

I. INTRODUCTION

Understanding of giant magnetoresistance (GMR) rests on an understanding of the size-dependent conductivity in thin-film multilayers. Most efforts to model the experimental conductivity of GMR multilayers (Co/Cu, NiFe/Ag, Fe/Cr, etc.) have assumed free-electron behavior within the constituent layers,[1] extending the Fuchs-Sondheimer approach.[2] Spin-dependent scattering, introduced through the spin dependence of some scattering parameters,[3,4] is considered in these models to be the source of GMR. The scattering at the ferromagnet/noble-metal interfaces is not assumed to be intrinsic, but may be introduced through separate parameters. Nevertheless, even if these parameters are included in semiclassical free-electron models, experimental conductivities tend to be underestimated for thick ferromagnetic layers and overestimated for thin ones.[5–7]

Several models of GMR exist which treat the band structure of the multilayers in a realistic fashion;[8–12] some of these[8,10] indicate that the electronic structure provides a source of GMR distinct from spin-dependent scattering. The conductivities calculated through realistic treatment of the multilayer band structure have not yet been compared in much detail with experiment. Butler *et al.* have compared experimental and theoretical conductivities for $\mathrm{Co}(t)/\mathrm{Cu}/\mathrm{Co}(t)$ spin valves as a function of one constituent layer thickness, fit with three empirical parameters.[14]

A very complete characterization of the multilayer conductance is provided by *in situ* conductance monitoring, which allows us to determine the full thickness-dependent film conductance $G(t)$ and infer the incremental conductance contributed by each atomic layer. This technique has been proposed recently as a process diagnostic for GMR spin-valve deposition;[15] at present, however, little understanding exists of how an ideal $G(t)$ curve should appear for even the simplest spin-valve structure, NiO/Co/Cu/Co. Comparison of experimental and theoretical $G(t)$ curves is thus of interest for both empirical and theoretical approaches to understanding GMR.

We present data on the full thickness-dependent conductivity $G(t_{\mathrm{tot}})$ of NiO/Co/Cu/Co spin-valve structures, measured *in situ* during ion-beam deposition. Good agreement is found with calculations based on realistic band structure using a single parameter for spin-independent disorder in Co and Cu. It is shown that unexpected features in the thickness-dependent conductance may be associated with scattering at the Co/Cu interfaces. Comparison with theory indicates that most of this interfacial scattering arises from band-structure differences between the ferromagnet and noble-metal layers.

II. EXPERIMENTAL METHOD

The sample sheet conductances were measured continuously during deposition, using lock-in ac measurements in the four-wire Van der Pauw geometry. $G(t)$ characteristics for a series of samples may be measured without breaking vacuum; formation of electrical contacts to the surface is accomplished through a special load-lock transfer mechanism. A detailed description of this technique is provided elsewhere;[16] some aspects are summarized here.

The electrical contacts to the sample surface are formed through four Au pads 1 mm×1 mm wide and 3000 Å thick, located at the corners of the 15 mm×15 mm substrate. The pads are formed in a separate deposition run by evaporation

of Cr(100 Å)/Au(3000 Å) through a shadow mask; substrates for the pad deposition are 4-in. thermally oxidized Si wafers coated with 400 Å NiO. The Si wafer is cleaved into coupons after pad deposition to avoid sputtering onto and conduction through the sample sides. Typical point-to-point resistances of the bare $Si/SiO_2/NiO$(/Au-contact) substrate, measured *in situ* immediately prior to spin-valve deposition, were 1 MΩ, with 0.5 MΩ measured in the four-wire geometry. Measurement and deposition take place at ambient temperature (300 K). A thermocouple located beneath the sample during similar depositions has shown very little temperature rise due to sputtering, with an increase of $<5\,°C$ recorded over 30 min continuous sputtering.

For this study, a series of NiO/Co(20)/Cu(t)/Co(50 Å) spin-valve structures in Cu thickness, $t=7.8$, 11.0, 15.5, 23.3 Å, was deposited and conductances measured *in situ*. To determine the periodicity of features observed, a NiO/Co(20)/$[$Cu(20)/Co(10 Å)$]_9$ multilayer was measured in comparison. All layers were formed by ion-beam sputtering in UHV with a base pressure of 2×10^{-9} torr, primary beam energy of 300 V, working Xe pressure of 4×10^{-4} torr, and beam current of 5.0 ± 0.1 mA. The NiO substrate was ion cleaned ($V_{beam}=300$ V, $P_{Ar}=4\times10^{-4}$ torr, 45-s duration) in vacuum immediately prior to deposition. Thicknesses were controlled by deposition time, calibrated by x-ray reflectivity measurements of layer thickness. A quartz microbalance has been used in some cases as secondary confirmation of deposition rate. No magnetic field has been applied and no exchange anisotropy introduced during deposition.

We have found in previous TEM investigation of ''bottom'' NiO-biased spin valves[17] that the deposited layers do not display any net preferred crystal orientation. The predominant growth mode of NiFe/Co/Cu/Co/NiFe on NiO in our system is such that there is local cube-on-cube epitaxy between randomly oriented fcc NiO grains and columnar grains formed by the NiFe/Co/Cu/Co/NiFe layers. We assume here that the bottom NiFe layer does not affect the epitaxy strongly, and that NiO/Co/Cu/Co exhibits similar crystalline ordering; this has been found to be the case in a HR-xTEM investigation of dc-magnetron sputtered NiO/Co/Cu/Co spin valves by Chopra *et al.*[18]

III. EXPERIMENTAL RESULTS

The full thickness-dependent conductivity data for NiO/Co(20)/Cu(t)/Co(50 Å) trilayers, $t=7.8$, 11.0, 15.5, 23.3 Å is presented in Fig. 1. Total film conductance measured *in situ* is plotted vs total layer thickness; the interface positions (Co on Cu, Cu on Co) are indicated by arrows. For Co on NiO, the onset of normal metallic film conductance is found at ~6 Å, approximately 3–4 ML coverage. The slope of the thickness-dependent conductance $G(t)$ increases gradually and approaches a more linear behavior up to 20 Å. This behavior is consistent with the formation of a high density of defects in the first several monolayers, causing a higher bulk layer resistivity, after which the layer quality is improved and lower layer resistivities are attained.

More striking features in conductance are observed at the interfaces. For Cu on NiO/Co(20 Å), a strong positive curvature is present in $G(t_{Cu})$: additional Cu layers contribute

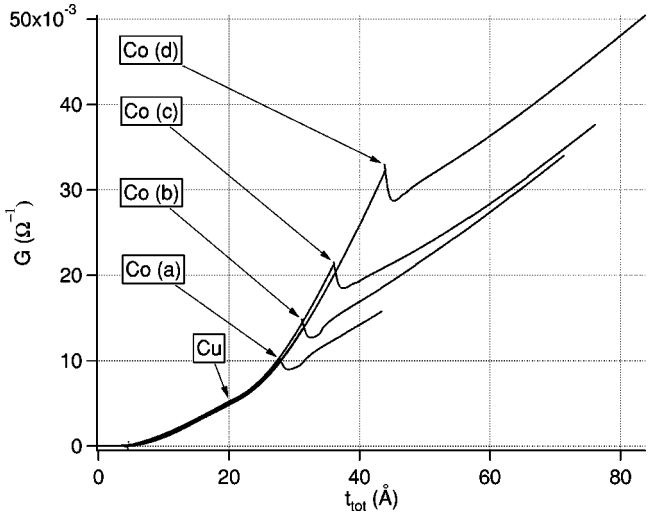

FIG. 1. Experimental film conductance $G(t_{tot})$ measured *in situ* during deposition of NiO/Co(20)/Cu(t_{Cu})/Co(40 Å) trilayers. The position of the interfaces (starting points for deposition of Cu and Co) is marked for samples A–D. $t_{Cu}=7.8$ Å (A), 11.0 Å (B), 15.5 Å (C), 23.3 Å (D). Note the strong deviations from linearity in the vicinity of the interfaces.

relatively little to the film conductance for low coverage, with progressively greater incremental contributions at greater thickness. We point out that the curvature in this plot is everywhere positive, with no kinks in the thickness-dependent conductance present. The incremental contributions to conductance are plotted in more detail in Fig. 2; these are plotted in their inverse units (resistivity) for easier comparison with tabulated values. We define the incremental resistivity as

$$\rho(t)=\left(\frac{\partial G(t)}{\partial t}\right)^{-1}.$$

The incremental resistivity may be identified with the bulk resistivity for the added layer only in the case where other

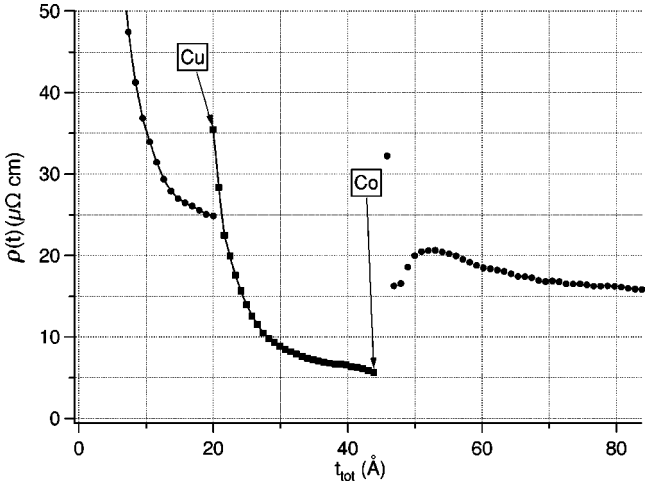

FIG. 2. Experimental incremental resistivity $\rho(t)$ for sample D. Note that the rapid decrease in effective resistivity with increasing Cu layer thickness is featureless. Saturation resistivities of 6 $\mu\Omega$ cm for Cu and 16 $\mu\Omega$ cm for Co are estimated.

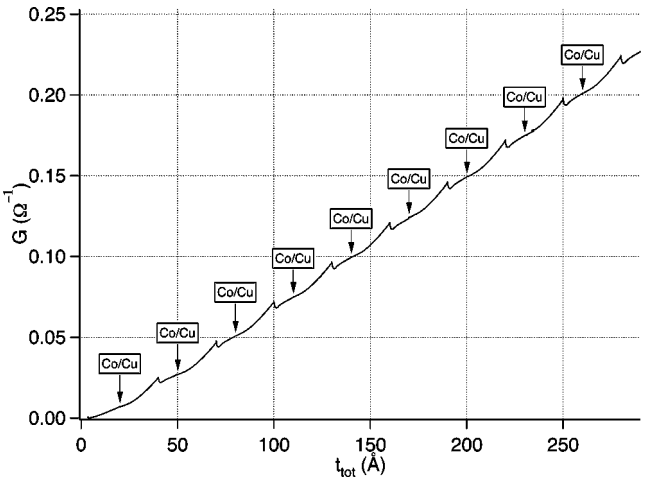

FIG. 3. Experimental film conductance $G(t_{\mathrm{tot}})$ measured *in situ* for a NiO/Co(20)/[Cu(20)/Co(10 Å)]$_9$ multilayer.

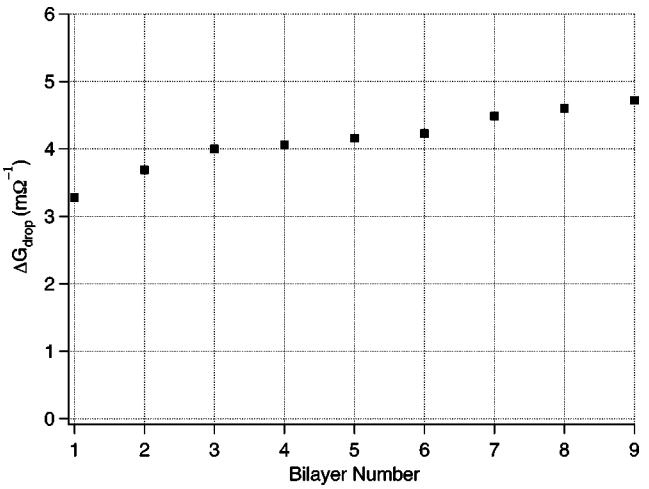

FIG. 4. Experimental conductance drop $\Delta G_{\mathrm{drop}}(N)$ produced in deposition of Co on Cu vs bilayer number N for the multilayer. An increasing trend in $\Delta G_{\mathrm{drop}}(N)$ with N is present.

defects (the bottom surface and interfaces) are several mean-free paths away. Otherwise, $\rho(t)$ should exceed the bulk resistivity for low-deposited thicknesses and gradually converge to the bulk value. From Fig. 2, we can see that the behavior of $G(t_{\mathrm{Cu}})$ converges towards linearity at ~20 Å Cu. If one is inclined to search for an enhancement in surface specularity, this could only be located in a rate of increase for $G(t_{\mathrm{Cu}})$, which is faster at low coverages than it is at high coverages. Some local minimum in $\rho(t)$ would need to be present, but it has not been observed.[21] We may identify the saturation rate of increase with an upper limit on the bulk resistivity of Cu, estimated at about 6 $\mu\Omega$ cm in this thickness range.

Deposition of submonolayer Co on NiO/Co(20 Å)/Cu produces, in all four cases, a drop in the total film conductance. This is surprising behavior given that a parallel conductor is being added. A strong Cu size dependence of the conductance drop magnitude is immediately apparent, with thicker Cu layers producing larger drops in conductance. The minimum conductance is reached at a coverage of ~1.2 Å Co. Some additional structure is visible at ~3 Å coverage. Roughly linear behavior is recovered thereafter; an initially higher slope may be attributed to scattering by disorder at the interface. An upper limit of 16 $\mu\Omega$ cm is estimated here for the bulk resistivity of Co.

To determine the repeatability of the thickness-dependent conductance features, we have also examined a NiO/Co(20)/[Cu(20)/Co(10 Å)]$_9$ multilayer. $G(t)$ data for the multilayer is presented in Fig. 3. The observed behavior for trilayers is indeed quite repetitive: always positive curvature in $G(t)$ for Cu(20 Å) on Co, always a conductance drop followed by a linear increase for Co(10 Å) on Cu. The features observed in Fig. 3 are quite similar to those observed in [NiFe(23)/Cu(20 Å)]$_8$ by Urbaniak, Lucinski, and Stobiecki,[22] but the interpretation of the data is quite different here (next section).

The conductance drops $\Delta G_{\mathrm{drop}}(N)$ are plotted as a function of bilayer number N in Fig. 4; in Fig. 5, $\Delta G_{\mathrm{drop}}(N)$ is plotted as a function of the Cu interlayer conductance $G(t_{\mathrm{Cu}})$. No decreasing trend is visible in $\Delta G_{\mathrm{drop}}(N)$; instead, the ΔG_{drop} depends primarily on the conductance of the Cu interlayer. These features will be discussed in Sec. V.

IV. COMPARISON WITH THEORY

The electronic structure of perfectly layered, (100)-oriented Co/Cu/Co trilayers has been calculated using a realistic multiband tight-binding model accounting for s, p, and d orbitals with their full hybridization and spin polarization. An advantage of the model is that the high levels of defects, principally grain boundaries, present in typical sputtered films may be treated using a physical parameter γ, where γ^2 within a layer corresponds to the mean-square variation in the onsite energy for an orbital. The parameter γ characterizes, in this case, the amount of bulk disorder within the multilayer. A detailed treatment of the model is provided in Ref. 12. The presence of increased interface disorder can be described by introducing a higher local value for the parameter γ for the respective interfacial layers in accordance with Ref. 13.

To fit the experimental resistivities, we have set $\gamma = 0.62$ eV for Cu and Co layers alike. Bulk resistivities are found of 5.9 $\mu\Omega$ cm for Cu and 14.8 $\mu\Omega$ cm and Co, in good

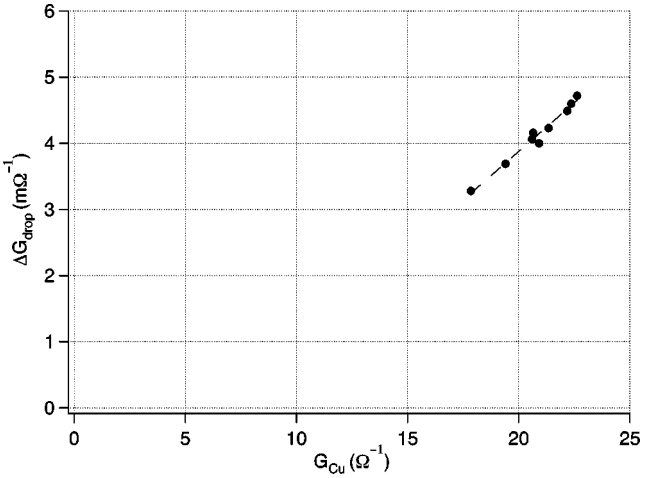

FIG. 5. Experimental ΔG_{drop} plotted against the Cu interlayer conductance $G(t_{\mathrm{Cu}})$ for the multilayer. Normalized to the Cu interlayer conductance G_{Cu}, the conductance drops are constant to within 0.15 mΩ^{-1} or ±4%.

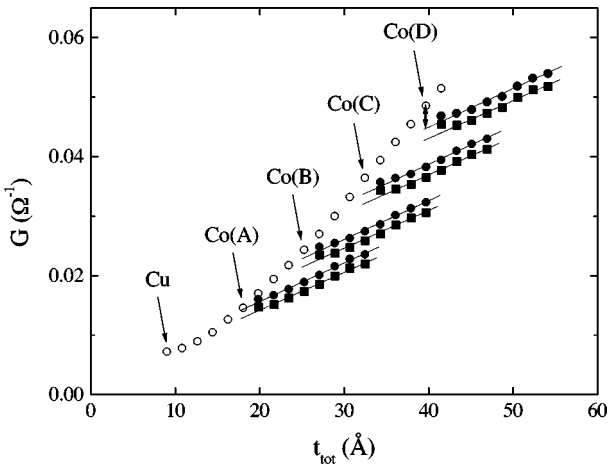

FIG. 6. Calculated $G(t_{\text{total}})$ data for Co(4 ML)/Cu(t_{Cu})/Co(8 ML). The position of the interfaces is marked for calculations A–E. $t_{\text{Cu}}=6$ ML (A), 10 ML (B), 14 ML (C), 18 ML (D). 1 ML Cu (100) = 1.80 Å. ○, calculations for Co(4 ML)/Cu(t_{Cu}) bilayers. ●, ■, calculations for Co(4 ML)/Cu(t_{Cu})/Co(t_{Co}) trilayers. Circles represent calculations with constant disorder parameter γ throughout the stack; squares represent calculations assuming increased γ at the top two Cu/Co interface layers. Note the strong deviations from linearity in the vicinity of the interfaces. Linear fits to the second Co layer data are indicated, used to determine ΔG_{drop}. The measurement of ΔG_{drop} for calculation D with constant disorder is indicated.

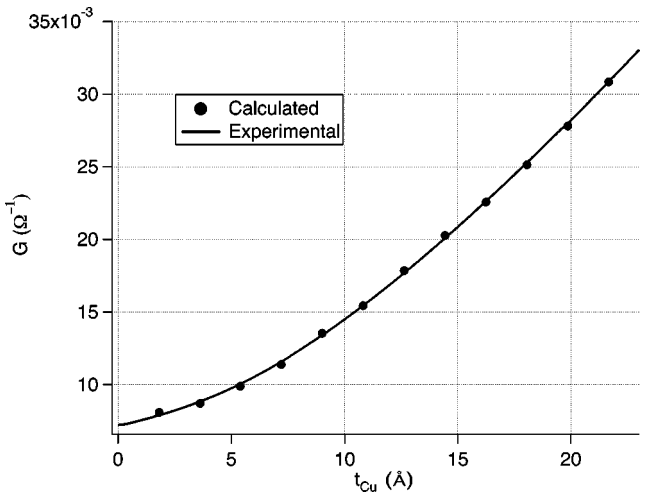

FIG. 7. Comparison of experimental and theoretical $G(t_{\text{Cu}})$. The experimental curve has been offset in G by $+2.3$ mΩ^{-1}.

agreement with both experimentally observed values at high-layer thickness (6 $\mu\Omega$ cm for Cu and 16 $\mu\Omega$ cm for Co). Numerous high-resolution cross-sectional transmission electron microscopy investigations of spin-valve microstructure, on samples deposited on our equipment[17,19] and elsewhere,[20] have shown little variation in grain size and crystallographic disorder across Cu and Co layers in GMR spin valves and multilayers. The fact that one empirically introduced level of disorder yields agreement with two experimental resistivities provides some confidence in the model calculation.

The qualitative features of the experiment are reproduced in the calculated conductances for Co(4 ML)/Cu(t)/Co(8 ML) trilayers, $t=6$, 10, 14, and 18 ML, shown in Fig. 6. There is a roughly linear increase in conductance for the initial Co layer (not shown). No attempt has been made to reproduce the gradual increase in conductance observed in the experiment up until ~15 Å Co; this behavior may be attributed straightforwardly to a high level of defects present in the first several monolayers of Co on NiO. Cu on Co produces a slow increase in $G(t)$, characterized by a strong positive curvature. Co on Cu produces an initial drop in conductance, followed by a roughly linear increase. The conductance drop seen for deposition of Co on Cu is size dependent in Cu thickness: larger drops in conductance are observed for thicker Cu layers.

A quantitative comparison of theory and experiment is presented in Figs. 7 and 8. In Fig. 7, we compare the experimental and calculated $G(t)$ for Co/Cu(t). Experimental and theoretical points are in close agreement. In Fig. 8, we compare the experimental and calculated conductance drop for the addition of Co to Co/Cu(t). For the experimental points, the drop is measured by taking the difference between the initial and minimum conductances (at ~1.2 Å Co); for the theoretical points, the drop is measured between G calculated for Co(4 ML)/Cu(t_{Cu}) and a linear extrapolation of G for Co(4 ML)/Cu(t_{Cu})/$G(t_{\text{Co}})$ curve back to zero t_{Co}. The measurement of ΔG_{drop} is indicated in Fig. 6 for the sample with the thickest Cu layer. Here we find that the experimental conductance drops exceed the calculated ones by a roughly constant value of 1.7 mΩ^{-1}.

The experimental and theoretical conductance drop values may be brought into agreement by introducing disorder at the top Cu/Co interface. In a second set of calculations, the addition of Co(1 ML) to Co/Cu(t) was assumed to create disorder in both layers forming the interface; we have modeled this interfacial disorder by setting $\gamma=0.80$ eV for the top two monolayers Cu(1 ML)/Co(1 ML) and $\gamma=0.62$ eV for the underlayers Co(4 ML)/Cu(t-1 ML) and the Co overlayers. Agreement between experiment and theory becomes quite close for this case.

The contributions of the various layers to total conductance G_n were calculated using the method described in Ref.

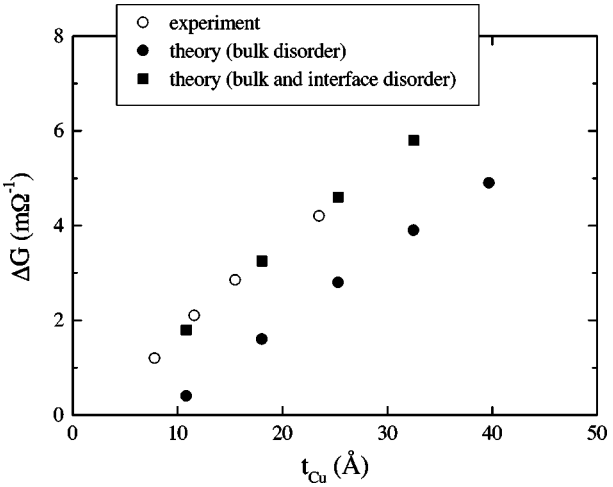

FIG. 8. Comparison of experimental and calculated ΔG_{drop}. The agreement is improved where additional disorder is introduced to the top Cu/Co interface in the calculation; this may be attributed to segregation of low surface energy Cu through Co in the experiment.

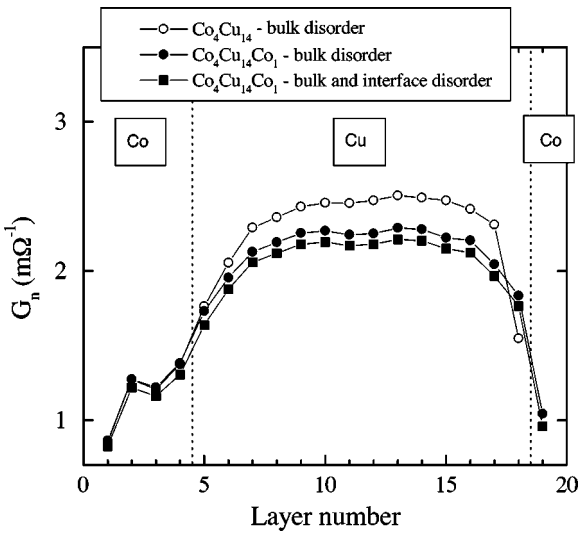

FIG. 9. Illustration of layer contributions to total conductance and ΔG_{drop}. Calculated points, $\gamma = 0.62$ eV: (a) Co/Cu bilayer (○), (b) Co/Cu bilayer with one monolayer Co at the surface (●), (c) same with disorder of the top two layers (18 and 19) increased to $\gamma = 0.80$ eV, reflecting surface segregation of Cu through Co. Note that where the bulk scattering is unchanged, the ΔG_{drop} is produced almost entirely within the Cu layer. The positions of the Co/Cu and Cu/Co interfaces are marked with dashed lines.

13. They are shown in Fig. 9, reflecting the contributions of various layers to ΔG_{drop}. Three calculations for the Co/Cu bilayer are presented. The first is a calculation for the bilayer alone and the second is for the bilayer covered by a monolayer of Co. In the first and second calculations the parameter γ was the same for all the layers, thereby representing bulk disorder. The third calculation is for the second structure with increased disorder at the top interface. A possible source for this disorder is surface-segregation of Cu through the Co, as will be discussed in Sec. V.

Several features are significant in Fig. 9. First, the ~4 ML of Cu near the bottom Co interface show significantly reduced conductance compared with layers in the bulk of the Cu. Second, when Co is added to the surface in the absence of increased disorder, the conductance is reduced exclusively within the Cu layers. These features point out the origin of the ΔG_{drop} and its t_{Cu} dependence: as the first several layers of Cu are already strongly reduced in conductance by the *d* states at the bottom interface with Co, layers further removed (at greater t_{Cu}) experience most of the effect from the added *d* states in the top layer. When additional disorder is introduced at the Cu/Co interface, on the other hand, the additional scattering contributions to ΔG_{drop} are balanced throughout the film stack. Finally, it is apparent that the calculation predicts slightly reduced conduction in the surface layers; this arises not from scattering, but instead from the change in band dispersion at the sites with reduced coordination number.

V. DISCUSSION

We have shown good agreement between the experimental and calculated film conductances in a model which considers only the differences in electronic structure between the layers, without assuming variations in the quality of the layers. Unexpected features in $G(t)$ for the trilayer are well described and may be rationalized simply through the difference in unoccupied *d* states for Cu and Co. The drop in conductance may be associated with the placement of a high density of unoccupied Co *d* states at the interface with Cu: the gradual increase in Cu conductivity may be attributed to the reduced influence of the same interfacial states as they move beyond the electronic mean-free path in Cu.

The conductance drop observed during deposition of Co on Cu has been attributed previously to a simple change in surface scattering character (''specularity'')[23] presumed to arise from an increase in the atomic-scale roughness of the surface. *In situ* resistance observation of conductance drops for Ni on Cu (Ref. 24) and $Ni_{80}Fe_{20}$ on Cu (Ref. 22) have been interpreted similarly. From the multilayer data, we may exclude surface-scattering variations as the principal source of the conductance drop. If the drops in conductance are interpreted through a simple application of the Fuchs-Sondheimer model as a reduction in the top surface specularity parameter p_{top}, this corresponds to $\Delta p_{\mathrm{top}} \sim -0.3$. Since the curvature in $G(t_{\mathrm{Cu}})$ is everywhere positive, converging to a value of bulk resistivity close to that observed up to ~150 Å thickness, we may not locate any complementary increase in specularity for Cu on Co. As only a net decrease in specularity may be inferred from Co/Cu bilayer depositions, the $\Delta G_{\mathrm{drop}}(N)$ should be exhausted after several bilayers when $p_{\mathrm{top}} = 0$. We have found that the drops are not at all exhausted over nine iterations: only an increasing trend may be inferred in $\Delta G_{\mathrm{drop}}(N)$. $\Delta G_{\mathrm{drop}}(N)$ becomes greater at greater thickness because of gradual improvements in the Cu layer quality, inferred through the higher conductance of the Cu interlayers. The Cu conductance thus becomes more sensitive to scattering at the boundaries by Co. We have modeled this effect in trilayers by increasing γ within Cu and examining the dependence of $\Delta G_{\mathrm{drop}}(N)$ on $G(t_{\mathrm{Cu}})$; a linear dependence of similar slope has been found.

For a more exact description of the experimental thickness-dependent conductance drops, we have found it necessary to assume some additional disorder for the top Cu/Co interface not present for the bottom Co/Cu interface or the rest of the stack. Segregation of low surface-energy Cu during coverage by Co may provide the driving force for such asymmetric interface intermixing: for segregation of Co through Cu, no surface free-energy reduction would be present. Segregation behavior is well documented in surface-analytical studies of Co on Cu single crystals of (100), (110), and (111) orientation.[25,26]

VI. CONCLUSION

We have interpreted the thickness-dependent conductance of NiO/Co/Cu/Co trilayer structures, measured *in situ* during deposition, in terms of intrinsic interface scattering. Both the strong positive curvature observed for $G(t_{\mathrm{Cu}})$ on Co and the conductance drop observed for $G(t_{\mathrm{Co}})$ on Cu may be attributed to scattering by the higher density of empty Co *d* states placed at the interface with Cu. No variations in extrinsic scattering need be introduced for a qualitative fit to the thickness-dependent conductance in the vicinity of the inter-

faces; a previous interpretation of the conductance drop in terms of surface-morphological scattering has been ruled out from $[Co/Cu]_9$ multilayer data. Quantitative agreement between a one-parameter theory, based on realistic band structure and incorporating the physical levels of disorder observed in typical films, and experiment is found for $G(t_{Cu})$ on NiO/Co. For $G(t_{Co})$ on NiO/Co/Cu, additional disorder at the top interface must be introduced for a quantitative fit, attributed to segregation of low surface energy Cu through Co.

ACKNOWLEDGMENT

This work was partially supported by the NSF/NSIC EHDR program.

*Present address: NIST, mail code 814.05, 325 Broadway, Boulder, CO 80303. Electronic address: baileyw@boulder.nist.gov URL: http://crism.stanford.edu/~web/

†Electronic address: sxwang@ee.stanford.edu

[1] R. Dimmich and F. Warkusz, Thin Solid Films **109**, 103 (1983).

[2] K. Fuchs, Proc. Cambridge Philos. Soc. **34**, 100 (1938); E. H. Sondheimer, Adv. Phys. **1**, 1 (1952).

[3] R. E. Camley and J. Barnas, Phys. Rev. Lett. **63**, 664 (1989).

[4] B. Dieny, J. Phys.: Condens. Matter **4**, 8008 (1992).

[5] C. Cowache, B. Dieny, A. Chamberod, D. Beniziri, F. Berthet, S. Auffret, L. Giacomoni, and S. Nossov, Phys. Rev. B **53**, 15 027 (1996).

[6] J. D. Jaratt, T. J. Klemmer, and J. A. Barnard, J. Appl. Phys. **81**, 5793 (1996).

[7] B. Dieny, V. S. Speriosu, J. P. Nozieres, B. A. Gurney, A. Vedayaev, and N. Ryzhanova, in *Magnetism and Structure in Systems of Reduced Dimension*, Vol. 309 of *NATO Advanced Study Institute, Series B: Physics*, edited by R. Farrow *et al.* (Plenum, New York, 1993).

[8] K. M. Schep, P. J. Kelly, and G. E. W. Bauer, Phys. Rev. Lett. **74**, 586 (1995).

[9] P. Zahn, I. Mertig, M. Richer, and H. Eshrig, Phys. Rev. Lett. **75**, 2996 (1995).

[10] W. H. Butler, X.-G. Zhang, D. M. C. Nicholsohn, T. C. Schulthess, and J. M. MacLaren, Phys. Rev. Lett. **76**, 3216 (1996).

[11] R. K. Nesbet, J. Phys.: Condens. Matter **8**, L569 (1996).

[12] E. Yu. Tsymbal and D. G. Pettifor, Phys. Rev. B **54**, 15 314 (1996).

[13] E. Yu. Tsymbal and D. G. Pettifor, J. Magn. Magn. Mater. **202**, 163 (1999).

[14] W. H. Butler, X.-G. Zhang, T. C. Schulthess, D. M. C. Nicholson, J. M. MacLaren, V. S. Speriosu, and B. A. Gurney, Phys. Rev. B **56**, 14 574 (1997).

[15] W. E. Bailey, C. Fery, K. Yamada, and S.-X. Wang, J. Appl. Phys. **85**, 7345 (1999).

[16] W. E. Bailey, C. Fery, K. Yamada, A. Wee, K. Sin, and S. X. Wang (unpublished).

[17] S. X. Wang, W. E. Bailey, and C. Surgers, IEEE Trans. Magn. **33**, 2369 (1997).

[18] H. D. Chopra, B. J. Hockey, P. J. Chen, W. F. Egelhoff, Jr., M. Wuttig, and S. Z. Hua, Phys. Rev. B **55**, 8390 (1996).

[19] W. E. Bailey, N-C. Zhu, R. Sinclair, and S-X. Wang, J. Appl. Phys. **79**, 6393 (1995).

[20] P. Bayle-Guillemaud, A. K. Petford-Long, T. C. Anthony, and J. A. Brug, IEEE Trans. Magn. **35**, 4627 (1996).

[21] Separate depositions (not shown) show that the established $\rho(t)$ at 20 Å is maintained up to 150 Å Cu.

[22] M. Urbaniak, T. Lucinski, and F. Stobiecki, J. Magn. Magn. Mater. **190**, 187 (1998).

[23] T. H. Eckl, G. Reiss, H. Bruckl, and H. Hoffmann, J. Appl. Phys. **75**, 362 (1994).

[24] H. Hoffmann, H. Hornauer, U. Jacob, and J. Vancea, Thin Solid Films **129**, 181 (1985); **131**, 1 (1985).

[25] M. T. Kief and W. F. Egelhoff, Jr., Phys. Rev. B **47**, 10 785 (1993).

[26] J. de la Figuera, J. E. Prieto, C. Ocal, and R. Miranda, Phys. Rev. B **47**, 13 043 (1993).